Contribution from the Departments of Chemistry, The University of North Carolina at Charlotte, Charlotte, North Carolina 28223, and The University of North Carolina at Chapel Hill, Chapel Hill, North Carolina 27514, and Chemistry Division, Oak Ridge National Laboratory, Oak Ridge, Tennessee 37830

# Structure and Redox and Photophysical Properties of a Series of Ruthenium Heterocycles Based on the Ligand 2,3-Bis(2-pyridyl)quinoxaline

D. Paul Rillema,*† Donna G. Taghdiri,† Daniel S. Jones,*† Charles D. Keller,† Laura A. Worl,‡ Thomas J. Meyer,*‡ and Henri A. Levy§

*Received July 7, 1986*

The synthesis, structure, and redox and photophysical properties of $[Ru(bpy)_n(BL)_{3-n}]^{2+}$, where $n = 0-2$, bpy is 2,2'-bipyridine, and BL is 2,3-bis(2-pyridyl)quinoxaline, are described. The $[Ru(bpy)_2(BL)](PF_6)_2$ complex crystallized in the monoclinic space group $P2_1/a$ with cell parameters of $a = 14.664$ (4) Å, $b = 16.345$ (5) Å, $c = 18.978$ (5) Å, $\beta = 100.19$ (2)°, and $Z = 4$. Data were collected on a Picker automated diffractometer using the $\theta-2\theta$ scan method. All non-H atoms were refined anisotropically to an $R$ value of 0.0672 for 5766 reflections with $I > \sigma(I)$. The ruthenium to nitrogen bond distances were Ru-N(pyridine) = 2.06 Å (average) and Ru-N(pyrazine) = 2.096 (4) Å. Absorption spectra contained bands (250-300 nm) in the ultraviolet region that were assignable to ligand $\pi \rightarrow \pi^*$ transitions and visible bands (517-300 nm) that were assignable to $d\pi \rightarrow \pi^*$ MLCT transitions. Reduction potentials for the $Ru^{3+/2+}$ couples varied from about 1.40 to 1.70 V vs. SSCE. Three reductions were observed and assigned to the one-electron reduction of each bidentate ligand, commencing with BL and then followed by bpy. Weak luminescence ($\Phi_r$ varied from 0.012 to 0.002 in 4:1 EtOH-MeOH) was observed, and corrected emission energy maxima were located at 766 ± 4 nm. Excited-state reduction potentials were estimated from the difference between emission energy maxima and ground-state reduction potentials. Potentials for excited-state $Ru^{2+*/+}$ couples ranged from 1.00 to 1.20 V; those of the $Ru^{3+/2+*}$ couples ranged from -0.12 to -0.39 V. Excited-state lifetimes at room temperature in 4:1 EtOH-MeOH ranged from 167 to <70 ns. Temperature-dependent-lifetime (90-298 K) data gave evidence for $\Delta E'$ values of 1100 ± 300 $cm^{-1}$. The temperature dependence was attributed to either the third MLCT state according to the localized-orbital model or the presence of a fourth CT state for $[Ru(bpy)_2BL]^{2+}$, since little photochemistry was found for it, and to the third and/or the fourth CT state and the dd state for both $[Ru(BL)_2(bpy)]^{2+}$ and $[Ru(BL)_3]^{2+}$. Emission spectral fitting suggested contributions to the spectral profile from medium-energy ring stretching modes and low-energy metal-ligand stretching vibrations. A plot of $E_{00}$ vs. $\Delta E_{1/2}$ for a series of ruthenium luminophores, where $\Delta E_{1/2} = E_{1/2}^{3+/2+} - E_{1/2}^{2+/+}$, was linear with a slope of 0.87 and a correlation coefficient of 0.97.

## Introduction

In recent work, we[1,2] and others[3-9] have shown that the properties of metal to ligand charge-transfer (MLCT) excited states can be controlled synthetically. A large body of information has accumulated on the photochemical and photophysical properties of MLCT excited states of $d^6$ transition metals, most notably for $Ru(bpy)_3^{2+}$ (bpy is 2,2'-bipyridine).[10-30] A complication arising for Ru-based systems is a photoinstability arising from thermal population of d-d excited states following MLCT excitation. Studies on mixed-ligand complexes have demonstrated that Ru-based MLCT excited-state properties can be varied considerably with a proper choice of ligands leading, for example, to control of the luminescence ($\pi\pi^*$ vs. MLCT)[3c] and to possibilities of controlling photochemical properties as well.[1]

We report here the results of a series of studies on the mixed-ligand ruthenium heterocycles $[Ru(bpy)_n(BL)_{3-n}]^{2+}$ ($n = 0-2$) based on the ligand 2,3-bis(2-pyridyl)quinoxaline (BL) shown in Figure 1; these studies give additional insight into the effect of ligand variations on properties of MLCT states.

## Experimental Section

**Materials.** $RuCl_3 \cdot 3H_2O$ and 2,2'-bipyridine were purchased commercially and used without further purification. Tetraethylammonium perchlorate (TEAP) was purchased from Southwestern Analytical Chemicals, Inc., dried under vacuum at 70 °C, and used without further purification. Acetonitrile for electrochemistry was chromatographic or pesticide grade and dried over 4-Å molecular sieves before use. All other chemicals were purchased commercially as reagent grade chemicals and were used without further purification. Nitrogen gas was prepurified grade and was found acceptable for use as delivered. Elemental analyses were carried out by Atlantic Microlab, Inc., Atlanta, GA.

**Preparation of Compounds.** $Ru(bpy)_2Cl_2 \cdot 2H_2O$[31] and $Ru(bpy)Cl_4$[32] were prepared by literature methods. The BL ligand, 2,3-bis(2-pyridyl)quinoxaline, and $[Ru(bpy)_2BL](PF_6)_2 \cdot H_2O$ were available from previous studies in our laboratory or were prepared by methods previously reported.[33a]

Crystals of $[Ru(bpy)_2BL](PF_6)_2$ suitable for X-ray studies were obtained by slow evaporation of an acetone solution. The recrystallized complex contained an acetone molecule as solvate and had the stoichiometry $[Ru(bpy)_2BL](PF_6)_2 \cdot CH_3COCH_3$.

† The University of North Carolina at Charlotte.
‡ The University of North Carolina at Chapel Hill.
§ Oak Ridge National Laboratory.

(1) Allen, G. H.; White, R. P.; Rillema, D. P.; Meyer, T. J. *J. Am. Chem. Soc.* **1984**, *106*, 2613.
(2) Kober, E. M.; Marshall, J. L.; Dressick, W. J.; Sullivan, B. P.; Caspar, J. V.; Meyer, T. *J. Inorg. Chem.* **1985**, *24*, 2755.
(3) (a) Juris, A.; Belser, P.; Barigelletti, F.; von Zelewski, A.; Balzani, V. *Inorg. Chem.* **1986**, *25*, 256. (b) Juris, A.; Barigelletti, F.; Balzani, V.; Belser, P.; von Zelewski, A. *Inorg. Chem.* **1985**, *24*, 202.
(4) (a) Reveco, P.; Schmehl, R. H.; Cherry, W. R.; Fronczek, F. R.; Selbin, J. *Inorg. Chem.* **1985**, *24*, 4078. (b) Cherry, W. R.; Henderson, L. J., Jr. *Ibid.* **1984**, *23*, 983.
(5) Wacholtz, W. F.; Auerbach, R. A.; Schmehl, R. H. *Inorg. Chem.* **1986**, *25*, 227.
(6) Crutchley, R. J.; Lever, A. B. P. *J. Am. Chem. Soc.* **1983**, *105*, 1170.
(7) Morris, D. E.; Ohsawa, Y.; Segers, D. P.; DeArmond, M. K.; Hanck, K. W. *Inorg. Chem.* **1984**, *23*, 3010.
(8) Kitamura, N.; Kawaniski, Y.; Tazuke, S. *Chem. Phys. Lett.* **1983**, *97*, 103.
(9) Ackerman, M. N.; Interrante, L. V. *Inorg. Chem.* **1984**, *23*, 3904.
(10) Meyer, T. J. *J. Phys. Chem.*, in press.
(11) (a) Demas, J. N.; Crosby, G. A. *J. Am. Chem. Soc.* **1971**, *93*, 2841. (b) Harrington, R. W.; Crosby, G. A. *J. Chem. Phys.* **1973**, *59*, 3468. (c) Hager, G. D.; Crosby, G. A. *J. Am. Chem. Soc.* **1975**, *97*, 7031. (d) Hager, G. D.; Watts, R. J.; Crosby, G. A. *Ibid.* **1975**, *97*, 7037. (e) Hipps, K. W.; Crosby, G. A.; *Ibid.* **1975**, *97*, 7042. (f) Crosby, G. A.; Elfring, W. *J. Phys. Chem.* **1976**, *80*, 2206. (g) Elfring, W. H., Jr.; Crosby, G. A. *J. Am. Chem. Soc.* **1981**, *103*, 2683.
(12) (a) Felix, F.; Ferguson, J.; Gudel, H. A.; Ludi, A. *J. Am. Chem. Soc.* **1980**, *102*, 4096. (b) Ferguson, J.; Herren, F. *Chem. Phys. Lett.* **1982**, *89*, 371. (c) Ferguson, J.; Herren, F.; McLaughlin, G. M. *Ibid.* **1982**, *89*, 376. (d) Ferguson, J.; Krausz, E. R. *Ibid.* **1983**, *76*, 45. (e) Krausz, E. *Ibid.* **1985**, *116*, 501.
(13) (a) Durham, B.; Caspar, J. V.; Nagle, J. K.; Meyer, T. J. *J. Am. Chem. Soc.* **1982**, *104*, 4803. (b) Kober, E. M.; Meyer, T. J. *Inorg. Chem.* **1982**, *21*, 3967. (c) Caspar, J. V.; Meyer, T. J. *J. Am. Chem. Soc.* **1983**, *105*, 5583. (d) Kober, E. M.; Meyer, T. J. *Inorg. Chem.* **1984**, *23*, 3877. (e) Kober, E. M.; Sullivan, B. P.; Meyer, T. J. *Ibid.* **1984**, *23*, 2098.
(14) (a) DeArmond, M. K. *Acc. Chem. Res.* **1974**, *7*, 309. (b) DeArmond, M. K.; Carlin, C. M.; Haung, W. L. *Inorg. Chem.* **1980**, *19*, 62. (c) Motten, A. G.; Hanck, K.; DeArmond, M. K. *Chem. Phys. Lett.* **1981**, *79*, 541. (d) Carlin, C. M.; DeArmond, M. K. *Ibid.* **1982**, *89*, 297. (e) Morris, D. E.; Hanck, K. W.; DeArmond, M. K. *J. Am. Chem. Soc.* **1983**, *105*, 3032. (f) Ohsawa, Y.; DeArmond, M. K.; Hanck, K. W.; Morris, D. E.; Whitten, D. G.; Neveux, P. E., Jr. *Ibid.* **1983**, *105*, 6522.
(15) Hipps, K. W. *Inorg. Chem.* **1980**, *19*, 1391.
(16) Ceulemans, A.; Vanquickenborne, G. *J. Am. Chem. Soc.* **1981**, *103*, 2238.
(17) Creutz, C.; Sutin, N. *J. Am. Chem. Soc.* **1976**, *98*, 6384.

0020-1669/87/1326-0578$01.50/0 

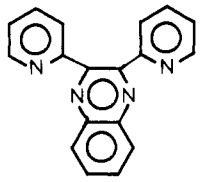

**Figure 1.** Structure of the ligand 2,3-bis(2-pyridyl)quinoxaline.

**$[Ru(BL)_3](PF_6)_2 \cdot 2H_2O$ and $[Ru(BL)_2(bpy)](PF_6)_2$.** Approximately 1 mmol of $Ru(bpy)Cl_4$ or $RuCl_3 \cdot 3H_2O$ was added to a twofold excess of BL needed to prepare the appropriate complex. The solids were suspended in 20 mL of ethylene glycol, and the resulting suspension was heated at reflux for 30 min. The solution was cooled to room temperature and then filtered to remove unreacted ligand. The volume of the filtrate was doubled by the addition of an equal volume of water, and the complex was then precipitated by the dropwise addition of a saturated aqueous $NH_4PF_6$ solution. The solid was collected by vacuum filtration, dissolved in a minimum amount of acetonitrile, precipitated by addition of the solution to ether, recollected by filtration, air-dried by suction, and then purified by chromatography.

The compound was redissolved in a minimum quantity of acetonitrile and added to a 40 mm diameter column containing neutral alumina to a depth of 10 cm. The column was developed and eluted with acetonitrile. The eluent was concentrated to ~10 mL and precipitation induced by addition to ether. The product was filtered and air-dried. The impurities that remained on the column were binuclear and oligonuclear complexes. No effort was made to remove or characterize them. These complexes were prepared directly via other methods, which will be described in a future publication. Anal. Calcd for $[Ru(BL)_3](PF_6)_2 \cdot 2H_2O$: C, 50.67; H, 3.15; N, 13.13. Found: C, 50.75; H, 2.84; N, 13.05. Calcd for $[Ru(BL)_2(bpy)](PF_6)_2$: C, 49.40; H, 2.88; N, 12.52. Found: C, 49.19; H, 2.96; N, 12.48.

**Physical Measurements.** Polarograms and/or cyclic voltammograms were obtained in acetonitrile at a Pt-disk working electrode with 0.1 M TEAP as the supporting electrolyte. The measurements were made vs. the saturated sodium calomel electrode (SSCE). Electrochemistry was carried out with a PAR 174 polarographic analyzer or the PAR 173 potentiostat in conjunction with a PAR 175 programmer. Polarograms were recorded with a Houston Omnigraphic X-Y recorder.

Visible-UV spectra were recorded with a Cary 14 spectrophotometer. Uncorrected emission spectra were obtained with a Hitachi Perkin-Elmer 650-40 spectrofluorimeter. Corrected emission spectra were obtained with an SLM Instruments, Inc., Model 800 photon-counting fluorescence instrument with stored correction factors. Emission quantum yields were determined in freeze-thaw-pump-degassed 4:1 EtOH-MeOH solutions at 25 °C by a relative method using an aqueous solution containing $[Ru(bpy)_3]^{2+}$ as the standard.[33b] The calculations used were based on eq 1,[29a,34] where $\Phi_{std}$ is 0.042 at $\lambda_{ex}$ = 436 nm, $A$ is the solution absorbance at 436 nm (<0.1), $I$ is the relative emission intensity, and $\eta$ is the index of refraction of the solvent.

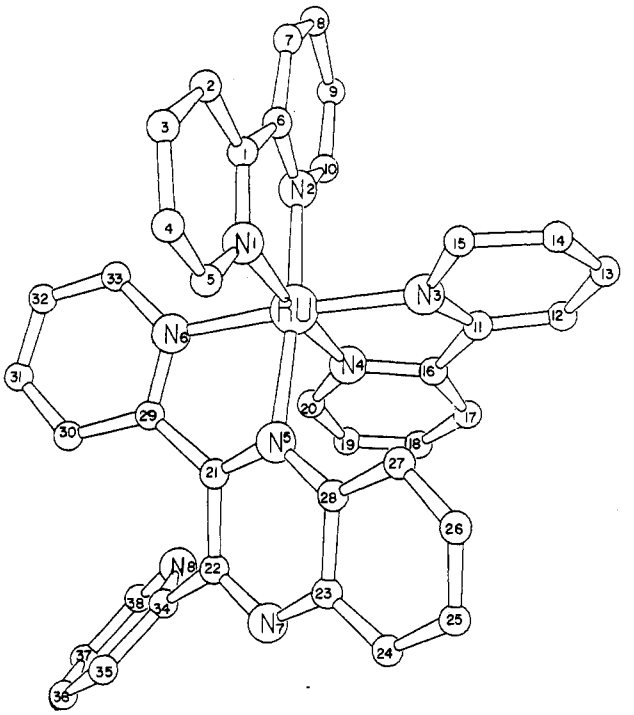

**Figure 2.** ORTEP drawing of the cation $[Ru(bpy)_2(BL)]^{2+}$.

$$\Phi_r = \Phi_{std} \frac{A_{std}}{A_r} \frac{I_r}{I_{std}} \frac{\eta_r^2}{\eta_{std}^2} \quad (1)$$

Lifetime measurements in 4:1 EtOH-MeOH were obtained by modification of methods described earlier.[13a] A Janis 6 NDT "Varitemp" liquid-nitrogen cryostat was utilized for temperature-dependence measurements. Room-temperature measurements were made with a water-jacketed sample cell constructed of Pyrex with two quartz windows located at right angles to one another. An Omega Engineering NaH-106-UU3553 thermistor was used to determine the temperature of the solutions.

Photochemical quantum yields were measured for the appropriate $Ru-BL^{2+}$ complex dissolved in acetonitrile containing 2 mM $[N(n\text{-}C_4H_9)_4]Cl$. The method described earlier for monitoring luminescence decay with time was used for the quantum-yield determinations.[13a]

**Kinetic and Spectral Fits.** Computer fits of temperature-dependent lifetime data were made with an algorithm supplied by Tektronix, Inc. The low-temperature emission spectra were corrected for slit-width variations as described by Parker and Reese prior to computer fits by a modified version of the fitting program written by Caspar.[35]

## Results and Discussion

**Preparation and Structure.** The preparation of $[Ru(bpy)_2BL](PF_6)_2$ was previously published along with that of the binuclear analogue $[Ru(bpy)_2]_2BL(PF_6)_4$.[33a] Preparation of $[Ru(BL)_2bpy](PF_6)_2$ and $[Ru(BL)_3](PF_6)_2$ followed procedures similar to those used to prepare the 2,2'-bipyrazine and 2,2'-bipyrimidine analogues.[36] The BL ligand is asymmetric, and structural isomers of $[Ru(BL)_2(bpy)](PF_6)_2$ and $[Ru(BL)_3](PF_6)_2$ are possible, but the spectral and redox properties described below fail to reveal difficulties associated with cis or trans isomers. An X-ray crystal structure determination of $[Ru(bpy)_2BL]^{2+}$ revealed that the $PF_6^-$ salt crystallized in space group $P2_1/a$ with $a$ =


(18) (a) Heath, G. A.; Yellowless, L. J.; Braterman, P. S. *Chem. Phys. Lett.* **1982**, *92*, 646. (b) Braterman, P.; Harriman, A.; Heath, G. A.; Yellowless, L. J. *J. Chem. Soc., Dalton Trans.* **1983**, 1801. (c) Braterman, P. S.; Heath, G. A.; Yellowless, L. J. *J. Chem. Soc., Dalton Trans.* **1985**, 1081.
(19) Cook, M. J.; Lewis, A. P.; McAuliffe, G. S. G.; Skarda, V.; Thomson, A. J. *J. Chem. Soc., Perkin Trans. 2*, **1984**, 1303.
(20) (a) Fujita, I.; Kobayashi, H. *Inorg. Chem.* **1973**, *12*, 2758. (b) Carlin, C. M.; DeArmond, M. K. *J. Am. Chem. Soc.* **1985**, *107*, 53.
(21) (a) Dallinger, R. F.; Woodruff, W. J. *J. Am. Chem. Soc.* **1979**, *101*, 4391. (b) Bradley, P. G.; Kress, N.; Hornberger, B. A.; Dallinger, R. F.; Woodruff, W. H. *Ibid.* **1981**, *103*, 7441. (c) McClanahan, S.; Hayes, T.; Kincaid, J. *Ibid.* **1983**, *105*, 4486. (d) Chung, Y. C.; Leventis, N.; Wagner, P. J.; Leroi, G. E. *Inorg. Chem.* **1985**, *24*, 1966.
(22) Smothers, W. K.; Wrighton, M. S. *J. Am. Chem. Soc.* **1983**, *105*, 1067.
(23) (a) Yersin, H.; Gallhuber, E.; Vogher, A.; Kunkely, H. *J. Am. Chem. Soc.* **1983**, *105*, 4155. (b) Yersin, H.; Gallhuber, E. *Ibid.* **1984**, *106*, 6582.
(24) Bugnon, P.; Hester, R. E. *Chem. Phys. Lett.* **1983**, *102*, 537.
(25) Elliott, C. M.; Hersenhart, E. J. *J. Am. Chem. Soc.* **1982**, *104*, 7519.
(26) Bensasson, R.; Salet, C.; Balzani, V. *J. Am. Chem. Soc.* **1976**, *98*, 3722.
(27) Krause, R. A.; Ballhausen, C. J. *Acta Chem. Scand., Ser. A* **1977**, *A31*, 535.
(28) Fetterolf, M. L.; Offen, H. W. *J. Phys. Chem.* **1985**, *89*, 3320.
(29) (a) Van Houten, J.; Watts, R. J. *J. Am. Chem. Soc.* **1976**, *98*, 4853. (b) Watts, R. J. *J. Chem. Educ.* **1983**, *60*, 834.
(30) Ollino, M.; Cherry, W. R. *Inorg. Chem.* **1985**, *24*, 1417.
(31) Sprintschnik, G.; Sprintschnik, H. W.; Whitten, D. G. *J. Am. Chem. Soc.* **1976**, *98*, 2337.
(32) Krause, R. A. *Inorg. Chim. Acta* **1977**, *22*, 209.
(33) (a) Rillema, D. P.; Mack, K. B. *Inorg. Chem.* **1982**, *21*, 3849. (b) Sullivan, B. P.; Salmon, D. J.; Meyer, T. J.; Peedrin, J. *Ibid.* **1979**, *18*, 3369.
(34) Guilbault, G. *Practical Fluorescence Theory, Methods and Techniques*; Marcel Dekker: New York, 1973; pp 11-14.
(35) Caspar, J. V.; Westmoreland, T. D.; Allen, G. H.; Bradley, P. G.; Meyer, T. J.; Woodruff, W. H. *J. Am. Chem. Soc.* **1984**, *106*, 3492. Caspar, J. V. Ph.D. Thesis, The University of North Carolina, Chapel Hill, NC, 1982.
(36) Rillema, D. P.; Allen, G.; Meyer, T. J.; Conrad, D. *Inorg. Chem.* **1983**, *22*, 1617.

**Table I.** Fractional Coordinates of Atoms with Estimated Standard Deviations[a]

| | x | y | z | | x | y | z |
|---|---|---|---|---|---|---|---|
| Ru | 0.80549 (3) | 0.95637 (3) | 0.78240 (2) | O | 0.5545 (5) | 0.0940 (5) | 0.3373 (5) |
| N1 | 0.6912 (3) | 1.0282 (3) | 0.7483 (2) | C39 | 0.6022 (10) | 0.0728 (8) | 0.3949 (8) |
| N2 | 0.7311 (3) | 0.9371 (2) | 0.8624 (2) | C40 | 0.6862 (9) | 0.0208 (8) | 0.3952 (10) |
| N3 | 0.7497 (3) | 0.8464 (3) | 0.7413 (2) | C41 | 0.5760 (15) | 0.1069 (14) | 0.4622 (10) |
| N4 | 0.9125 (3) | 0.8753 (3) | 0.8190 (2) | P1 | 0.6483 (1) | 1.1605 (1) | 1.0179 (1) |
| N5 | 0.8892 (3) | 0.9858 (2) | 0.7072 (2) | F1 | 0.6838 (3) | 1.2169 (3) | 0.9615 (3) |
| N6 | 0.8735 (3) | 1.0592 (2) | 0.8261 (2) | F2 | 0.6111 (3) | 1.1041 (3) | 1.0736 (3) |
| C1 | 0.6245 (3) | 1.0242 (3) | 0.7899 (3) | F3 | 0.5718 (3) | 1.1252 (2) | 0.9556 (2) |
| C2 | 0.5459 (5) | 1.0728 (4) | 0.7741 (4) | F4 | 0.7208 (3) | 1.1987 (3) | 1.0810 (2) |
| C3 | 0.5353 (5) | 1.1245 (5) | 0.7166 (4) | F5 | 0.7194 (3) | 1.0915 (2) | 1.0053 (2) |
| C4 | 0.6032 (5) | 1.1290 (5) | 0.6753 (4) | F6 | 0.5768 (3) | 1.2295 (2) | 1.0298 (2) |
| C5 | 0.6795 (5) | 1.0790 (4) | 0.6913 (4) | P2 | 0.8621 (1) | 0.2119 (1) | 0.5854 (1) |
| C6 | 0.6446 (4) | 0.9704 (4) | 0.8521 (3) | F7 | 0.8552 (3) | 0.2205 (3) | 0.5032 (2) |
| C7 | 0.5856 (4) | 0.9563 (4) | 0.8997 (3) | F8 | 0.8694 (4) | 0.2034 (3) | 0.6693 (3) |
| C8 | 0.6129 (4) | 0.9090 (4) | 0.9589 (4) | F9 | 0.8578 (4) | 0.1159 (2) | 0.5782 (2) |
| C9 | 0.7008 (5) | 0.8764 (3) | 0.9695 (3) | F10 | 0.8655 (3) | 0.3080 (3) | 0.5937 (3) |
| C10 | 0.7577 (4) | 0.8909 (4) | 0.9211 (3) | F11 | 0.9702 (3) | 0.2073 (4) | 0.5971 (3) |
| C11 | 0.8062 (4) | 0.7806 (4) | 0.7542 (3) | F12 | 0.7544 (3) | 0.2153 (4) | 0.5765 (3) |
| C12 | 0.7774 (6) | 0.7034 (3) | 0.7324 (4) | H2 | 0.4991 | 1.0704 | 0.8028 |
| C13 | 0.6882 (5) | 0.6924 (3) | 0.6952 (4) | H3 | 0.4815 | 1.1577 | 0.7057 |
| C14 | 0.6307 (5) | 0.7583 (5) | 0.6819 (4) | H4 | 0.5963 | 1.1655 | 0.6357 |
| C15 | 0.6617 (4) | 0.8334 (4) | 0.7062 (3) | H5 | 0.7261 | 1.0809 | 0.6624 |
| C16 | 0.8994 (4) | 0.7978 (3) | 0.7934 (3) | H7 | 0.5251 | 0.9792 | 0.8922 |
| C17 | 0.9722 (4) | 0.7412 (3) | 0.8060 (4) | H8 | 0.5724 | 0.8992 | 0.9919 |
| C18 | 1.0559 (5) | 0.7655 (4) | 0.8453 (4) | H9 | 0.7209 | 0.8436 | 1.0106 |
| C19 | 1.0682 (4) | 0.8422 (5) | 0.8719 (3) | H10 | 0.8181 | 0.8679 | 0.9285 |
| C20 | 0.9956 (4) | 0.8947 (4) | 0.8574 (3) | H12 | 0.8179 | 0.6579 | 0.7421 |
| C21 | 0.9606 (3) | 1.0337 (3) | 0.7344 (3) | H13 | 0.6669 | 0.6396 | 0.6790 |
| C22 | 1.0448 (4) | 1.0322 (3) | 0.7056 (3) | H14 | 0.5694 | 0.7508 | 0.6565 |
| N7 | 1.0503 (3) | 0.9919 (3) | 0.6467 (3) | H15 | 0.6212 | 0.8790 | 0.6974 |
| C23 | 0.9735 (4) | 0.9527 (4) | 0.6117 (3) | H17 | 0.9640 | 0.6870 | 0.7878 |
| C24 | 0.9775 (5) | 0.9128 (4) | 0.5492 (3) | H18 | 1.1060 | 0.7279 | 0.8544 |
| C25 | 0.9021 (6) | 0.8716 (5) | 0.5138 (4) | H19 | 1.1262 | 0.8579 | 0.8993 |
| C26 | 0.8200 (6) | 0.8723 (5) | 0.5420 (4) | H20 | 1.0040 | 0.9488 | 0.8756 |
| C27 | 0.8141 (5) | 0.9083 (4) | 0.6044 (3) | H24 | 1.0330 | 0.9140 | 0.5300 |
| C28 | 0.8923 (4) | 0.9480 (4) | 0.6420 (3) | H25 | 0.9059 | 0.8446 | 0.4701 |
| C29 | 0.9457 (3) | 1.0833 (3) | 0.7956 (3) | H26 | 0.7664 | 0.8452 | 0.5174 |
| C30 | 0.9947 (5) | 1.1549 (3) | 0.8197 (3) | H27 | 0.7581 | 0.9065 | 0.6229 |
| C31 | 0.9720 (5) | 1.1980 (4) | 0.8757 (3) | H30 | 1.0449 | 1.1733 | 0.7984 |
| C32 | 0.8986 (4) | 1.1718 (3) | 0.9056 (3) | H31 | 1.0059 | 1.2456 | 0.8931 |
| C33 | 0.8512 (4) | 1.1039 (4) | 0.8800 (3) | H32 | 0.8817 | 1.2021 | 0.9440 |
| C34 | 1.1331 (3) | 1.0667 (3) | 0.7450 (3) | H33 | 0.8004 | 1.0863 | 0.9010 |
| C35 | 1.1833 (4) | 1.1255 (4) | 0.7174 (4) | H35 | 1.1620 | 1.1492 | 0.6718 |
| C36 | 1.2654 (5) | 1.1515 (5) | 0.7571 (4) | H36 | 1.3012 | 1.1928 | 0.7396 |
| C37 | 1.2955 (5) | 1.1166 (5) | 0.8227 (4) | H37 | 1.3525 | 1.1339 | 0.8506 |
| C38 | 1.2427 (5) | 1.0577 (5) | 0.8451 (4) | H38 | 1.2638 | 1.0330 | 0.8904 |
| N8 | 1.1618 (3) | 1.0323 (3) | 0.8083 (2) | | | | |

[a] H positions are calculated.

14.664 (4) Å, $b$ = 16.345 (5) Å, $c$ = 18.978 (5) Å, $\beta$ = 100.19 (2)°, and $Z$ = 4. X-ray data were collected at Oak Ridge National Laboratory; observations were measured with Mo K$\alpha$ radiation to a 2$\theta$ value of 55°. Refinement led to an $R$ value of 0.0672 for 5766 reflections with intensities greater than the standard error of measurement.[37a] Positional parameters are given in Table I; Figure 2 shows an ORTEP[37b] drawing of the cation. The average Ru–N(pyridine) bond distance is 2.06 Å, and the Ru–N(pyrazine) bond distance is 2.096 (4) Å. Within the BL ligand, the angle between the plane of the pyrazine ring and the plane of the coordinated pyridine ring is 24°, and the N–C–C′–N′ torsional angle between these two rings is 16°. The angle between the plane of the coordinated pyridine ring and the plane of the remote pyridine ring is 66°. The $PF_6^-$ ions have nearly octahedral symmetry with an average P–F distance of 1.57 Å.

The Ru–N bond distances are close to the value, 2.06 Å, found in $[Ru(bpy)_3]^{2+}$ [38] with the exception of the longer Ru–N bond distance to the pyrazine moiety. The longer bond distance is in accord with the weaker $\sigma$ donor strength of the pyrazine group ($pK_a$ = 0.8)[39] compared to that of the pyridine ($pK_a$ = 5.23) unit.[40a] Steric factors may also play a role. The C(27) and H(27) atoms, on the basis of a C–H bond length of 0.95 Å, are within van der Waals contact of the N(3) and C(15) atoms of the neighboring bipyridine ring. The C(27)–N(3) distance is 3.09 Å, the C(27)–C(15) distance is 3.43 Å, the calculated H(27)–N(3) distance is 2.48 Å, and the calculated H(27)–C(15) distance is 2.59 Å. van der Waals radii are 1.55 Å for N, 1.65–1.70 Å for C, and 1.20–1.40 Å for H.[40b] Thus, the van der Waals contact distances are as follows: C to C, 3.30–3.40 Å; C to N, 3.20–3.25 Å; C to H, 2.85–3.10 Å; N to H, 2.75–2.95 Å. The longer bond distance

(37) (a) Data were collected on a Picker automated diffractometer using the $\theta$–2$\theta$ scan method. A total of 10 346 unique reflections were measured to a 2$\theta$ value of 55°; data were corrected for absorption. Refinement was carried out by varying a scale factor and positional and anisotropic thermal parameters for all non-H atoms. H positions were calculated, and H atoms were assigned the thermal parameters of the carbon atoms to which they were bonded. (Each H atom was placed 0.95 Å from its attached C atom, on a line from the ring center through the C atom.) No extinction corrections were made. Each asymmetric unit contained one acetone solvent molecule (O, C39, C40, C41), (b) Johnson, C. K. "Oak Ridge Thermal Ellipsoid Program"; ORNL Report No. 5138; Oak Ridge National Laboratory: Oak Ridge, TN, 1976.

(38) Rillema, D. P.; Jones, D. S.; Levy, H. *J. Chem. Soc., Chem. Commun.* **1979**, *849*.

(39) Ford, P.; Rudd, D. P.; Gaunder, R.; Taube, H. *J. Am. Chem. Soc.* **1968**, *90*, 1187.

(40) (a) *Handbook of Chemistry and Physics*, 42nd ed.; CRC: Boca Raton, FL, 1960; p 1750. (b) Huheey, J. E. *Inorganic Chemistry*, 3rd ed.; Harper & Row: New York, 1983; p 258.

**Table II.** Visible–UV Spectra of Ruthenium(II) Parent Complexes and Mixed-Ligand Complexes in Acetonitrile[a]

| compd | $d\pi \rightarrow \pi_1^*$(BL) | $d\pi \rightarrow \pi_1^*$(bpy) | $d\pi \rightarrow \pi_2^*$ | $\pi \rightarrow \pi^*$ |
|---|---|---|---|---|
| $[Ru(BL)_3]^{2+}$ | 499 ($1.4 \times 10^4$) | | 470 (sh), 392 (sh) | 325 ($4.0 \times 10^4$), 275 ($7.8 \times 10^4$) |
| $[Ru(BL)_2(bpy)]^{2+}$ | 512 ($9.6 \times 10^3$) | 462 ($8.3 \times 10^3$) | 390 (sh) | 330 (sh), 281 ($6.9 \times 10^4$), 256 (sh) |
| $[Ru(bpy)_2(BL)]^{2+}$ | 517 ($8.4 \times 10^3$) | 426 ($8.7 \times 10^3$) | 391 (sh), 350 (sh) | 325 (sh), 284 ($7.0 \times 10^4$) |
| $[Ru(bpy)_3]^{2+}$ [b] | | 451 ($1.4 \times 10^4$) | 345 ($6.5 \times 10^3$), 323 ($6.5 \times 10^3$) | 285 ($8.7 \times 10^4$), 250 ($2.5 \times 10^4$), 238 ($3.0 \times 10^4$) |

[a] $\lambda_{max}$ values are in nm, with error ±1 nm; $\epsilon$ values follow in parentheses with units in $M^{-1}$ $cm^{-1}$. $T = 20 \pm 1$ °C. [b] From: Crutchley, R. J.; Lever, A. B. P. *Inorg. Chem.* **1982**, *21*, 2276.

**Table III.** Polarographic Half-Wave Potentials for Ruthenium(II) Parent and Mixed-Ligand Complexes[a,b]

| compd | oxidn | redn | | | | |
|---|---|---|---|---|---|---|
| | $E_{1/2}$ | $E_{1/2}(1)$ | $E_{1/2}(2)$ | $E_{1/2}(3)$ | $E_{1/2}^{3+/2+*}$ [c] | $E_{1/2}^{2+*/+}$ [c] |
| $[Ru(BL)_3]^{2+}$ | 1.70 | −0.60 | −0.78 | −1.04 | −0.12 | 1.22 |
| $[Ru(BL)_2(bpy)]^{2+}$ | 1.53 | −0.66 | −0.89 | −1.58 | −0.25 | 1.12 |
| $[Ru(bpy)_2(BL)]^{2+}$ | 1.39 | −0.78 | −1.45 | *d* | −0.39 | 1.00 |
| $[Ru(bpy)_3]^{2+}$ [e] | 1.27 | −1.31 | −1.50 | −1.77 | −0.86 | 0.86 |
| BL | | −1.56 | | | | |

[a] Potentials are in V vs. SSCE. [b] Conditions: solutions 0.10 M in TEAP; solvent acetonitrile; $T = 25 \pm 1$ °C. [c] Calculated as in text using $E_{00}$ values from Table VI in eV. [d] An adsorption wave interfered with the determination of this potential. [e] Rillema, D. P.; Allen, G.; Meyer, T. J.; Conrad, D. *Inorg. Chem.* **1983**, *22*, 1617–1622.

suggests that the ligand field strength of the BL ligand is weaker than that of the bpy ligand, which should affect the $d\pi(t_{2g})$–$d\sigma^*(e_g)$ splitting, perhaps lowering the $\sigma^*$-based dd state relative to that of $[Ru(bpy)_3]^{2+}$.

The other structural feature of interest is the orientation of the remote pyridine ring. The fact that the ring is skewed with respect to the plane of ligand coordination accounts for the greater difficulty associated with formation of the binuclear complex than that of its mononuclear analogue.[33a] In order to form the binuclear complex, the ring must assume a near-planar orientation with respect to the other ligand components.

**Electronic Spectra.** The visible spectra of the Ru–$BL^{2+}$ series are shown in Figure 3. The absorption manifold of $[Ru(BL)_3]^{2+}$ is red shifted by ~45 nm compared to the manifold for $[Ru(bpy)_3]^{2+}$ but has a similar profile, indicating that similar assignments for the absorptions can be made. It is also interesting to note that the distinction between the MLCT transition involving the two different ligands is clear, with the $d\pi \rightarrow \pi^*$(BL) transitions occurring at lower energy than the analogous $d\pi \rightarrow \pi^*$(bpy) transitions. For $[Ru(bpy)_3]^{2+}$ itself, there are a series of $d\pi \rightarrow \pi^*$ transitions.[12a,13b] The first set, which consists of several transitions, involves excitations to the lowest $\pi^*$(bpy) level, $\pi_1^*$, and a second set approximately 6000 $cm^{-1}$ higher in energy involves transitions assigned as $d\pi \rightarrow \pi_2^*$. In mixed-ligand complexes the spectra are more complex. For the series $[Ru(bpy)_n(bpz)_{3-n}]^{2+}$ and $[Ru(bpy)_n(bpm)_{3-n}]^{2+}$ ($n = 1$–3; bpz is 2,2′-bipyrazine; bpm is 2,2′-bipyrimidine), it was possible to assign $d\pi \rightarrow \pi^*$ transitions from the metal center to the various ligands in the complexes.[36] For the mixed bpy–BL complexes, the lowest energy absorption feature can be assigned to $d\pi \rightarrow \pi_1^*$(BL) followed by $d\pi \rightarrow \pi_1^*$(bpy) and then by $d\pi \rightarrow \pi_2^*$ bands appearing as shoulders on the ligand-based $\pi$–$\pi^*$ bands.[12a,41] The $d\pi \rightarrow \pi_1^*$(bpy) transitions are expected to occur in the 400–450-nm region of the spectrum in accord with those of $[Ru(bpy)_3]^{2+}$ and blue shift with ligand replacement as found in other related systems.[1] The visible–UV assignments are summarized in Table II.

**Electrochemical Properties.** Redox properties are summarized in Table III. $E_{1/2}$ values were determined from peak currents of differential pulse polarograms and by cyclic voltammetry. The two techniques give complementary results. The differences in peak positions $\Delta E_p$, $\Delta E_p = E_{p(ox)} - E_{p(red)}$, for cyclic voltammograms were scan-rate dependent. Plots of the square root of the sweep rate vs. $\Delta E_p$ gave intercepts that varied from 60 to 70 mV, indicative of reversible one-electron-transfer processes.[42]

The uncoordinated ligand is reduced at −1.56 V whereas the coordinated ligand in $[Ru(BL)_3]^{2+}$ is reduced at −0.60 V vs. SSCE.

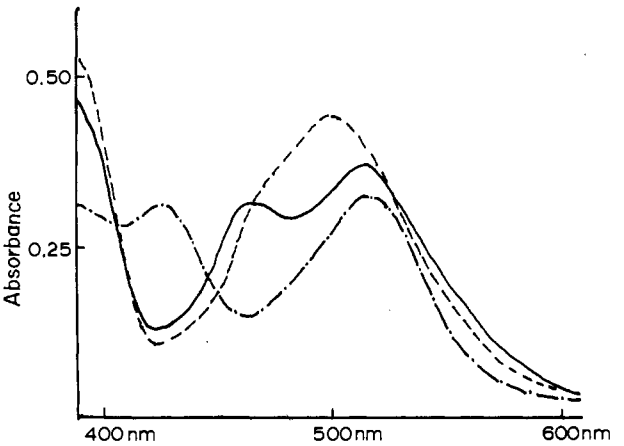


**Figure 3.** Visible spectra of the Ru–BL cations in acetonitrile: (---) $[Ru(BL)_3]^{2+}$; (—) $[Ru(BL)_2(bpy)]^{2+}$; (-·-) $[Ru(bpy)_2(BL)]^{2+}$. Equivalent concentrations of $3.5 \times 10^{-5}$ M in complex were used.

This observation is consistent with data for ruthenium heterocyclic complexes where the free ligand is reduced at ~1 V more negative than when coordinated to ruthenium(II). A plot of $E_{1/2}$ for reduction of the ligands bpy (−2.21 V), bpm (−1.99 V), bpz (−1.76 V), and BL (−1.56 V) vs. those values of the $Ru^{2+/+}$ couple in the tris heterocyclic complexes $[Ru(bpy)]^{2+/+}$ (−1.31 V), $[Ru(bpm)_3]^{2+/+}$ (−0.91 V), $[Ru(bpz)_3]^{2+/+}$ (−0.68 V), and $[Ru(BL)_3]^{2+/+}$ (−0.60 V) is linear with a slope of 1. The ligands chosen for the correlation are representative of a large number available and cover a rather wide range in potential (~0.5 V; from −1.56 to −2.21 V).

Three sequential reductions occur for $[Ru(BL)_3]^{2+}$, suggesting that each ligand is reduced consecutively.[2] In the case of mixed-ligand complexes, reduction occurs first at the ligand having the lowest $\pi^*$ levels and the sequential pattern of reduction for $[Ru(BL)_2bpy]^{2+}$ is

$$[Ru(bpy)(BL)(BL)]^{2+} + e^- \rightleftarrows [Ru(bpy)(BL)(BL^-)]^+ \quad (2)$$

$$E_{1/2} = -0.66 \text{ V}$$

$$[Ru(bpy)(BL)(BL^-)]^+ + e^- \rightleftarrows [Ru(bpy)(BL^-)(BL^-)] \quad (3)$$

$$E_{1/2} = -0.89 \text{ V}$$

$$[Ru(bpy)(BL^-)(BL^-)] + e^- \rightleftarrows [Ru(bpy^-)(BL^-)(BL^-)]^- \quad (4)$$

$$E_{1/2} = -1.58 \text{ V}$$

A plot of $E_{1/2}$ for the $Ru^{3+/2+}$ couple vs. $E_{1/2}$ for the first reduction of each complex is linear with a slope of 1.6. The linearity results from the fact that the $\pi^*$ levels are lowered in

(41) Rillema, D. P.; Callahan, R. W.; Mack, K. B. *Inorg. Chem.* **1982**, *21*, 2589.
(42) Nicholson, R. S.; Shain, I. *Anal. Chem.* **1964**, *36*, 705.

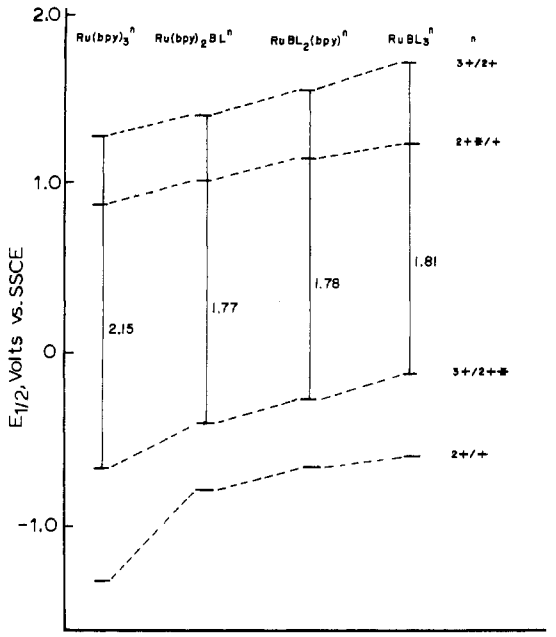


**Figure 4.** Redox potential diagram comparing excited-state and ground-state reduction potentials. The latter were estimated on the basis of the difference in energy of $E_{00}$ (eV) from Table VI and potentials for the ground-state couples.

**Table IV.** Room-Temperature Emission Maxima, Quantum Yields, Excited-State Lifetimes, and Substitution Quantum Yields[a]

| compd[b] | $\lambda_{em}$(max),[c] nm | $\tau_0$,[d] ns | $\Phi_r$[e] | $\Phi_p$[f] |
|---|---|---|---|---|
| $[Ru(BL)_3]^{2+}$ | 762 (714) | 70 | 0.012 | 0.029 |
| $[Ru(BL)_2(bpy)]^{2+}$ | 767 (734) | 167 | 0.010 | $7.6 \times 10^{-4}$ |
| $[Ru(bpy)_2(BL)]^{2+}$ | 770 (760) | ≤20 | 0.002 | $<10^{-4}$ |
| $[Ru(bpy)_3]^{2+}$[g] | 622 (620) | 800 | 0.040 | 0.0021[h] |

[a] Conditions: 25 ± 1 °C; determined in 4:1 ethanol–methanol solution. [b] $PF_6^-$ salts. [c] Correlated value followed by uncorrected value in parentheses. [d] Freeze–thaw–pump degassed. [e] $\lambda_{ex}$ = 436 nm, wavelength of maximum light source intensity. [f] Quantum yield for ligand loss in $CH_3CN$ containing 2 mM $[N(n\text{-}C_4H_9)_4]Cl$. [g] Dressick, W. J. Ph.D. Thesis, The University of North Carolina, 1981; p 151. [h] Ross, H. B.; Rillema, D. P., unpublished observations.

energy as the number of BL ligands increase and the lowered $\pi^*$ levels result in enhanced $d\pi \rightarrow \pi^*$ interaction.

For MLCT excited states, where excited-state distortion is relatively small, excited-state redox potentials can be estimated from ground-state redox potentials and the excited-state emission energy by $E_{1/2}{}^{3+/2+*} = E_{1/2}{}^{3+/2+} - E_{em}$ and $E_{1/2}{}^{2+*/+} = E_{1/2}{}^{2+/+} + E_{em}$.[43] The results of the calculations are tabulated in Table III, and the effects of the substitution of BL for bpy are illustrated in Figure 4. Values for the $Ru^{3+/2+*}$ couple vary from −0.12 to −0.39 V and from 1.00 to 1.22 V for the $Ru^{2+*/+}$ couple. The data indicate that the $Ru\text{–}BL^{2+*}$ complexes are poor reductants relative to $[Ru(bpy)_3]^{2+*}$ due to low-energy $\pi^*$ levels but are good oxidants due to enhanced $d\pi\text{–}\pi^*$ interactions.

**Luminescence Lifetimes, Quantum Yields, and Photochemical Quantum Yields.** Optical excitation by visible or UV light gives rise to luminescence decay similar to that of $[Ru(bpy)_3]^{2+*}$. For the series $[Ru(bpy)_n(BL)_{3-n}]^{2+}$, uncorrected emission maxima in acetonitrile are located at 714, 734, and 760 nm for $n$ = 0, 1, and 2, compared to 620 nm for $[Ru(bpy)_3]^{2+}$. For the sequence, excited-state lifetimes were 300, 405, and <20 ns in nitrogen-degassed acetonitrile solutions. Corrected luminescence maxima, excited-state lifetimes, and radiative quantum yields determined in 4:1 EtOH–MeOH are listed in Table IV. In contrast to the results in $CH_3CN$, the emission energies are relatively invariant

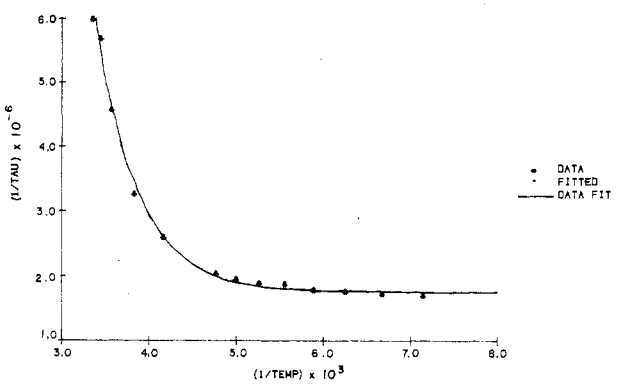


**Figure 5.** Comparison of the experimental lifetime data (*) with a computer-generated fit using eq 6 and the parameters in Table V for the couples of $[Ru(BL)_2(bpy)]^{2+}$. This figure covers the temperature range 150–298 °C and does not show the glass transition.

throughout the series. All are weak emitters and are relatively short lived.

The emission quantum yield dependence was examined over the spectral region of 400–530 nm in the temperature range 93–143 K for the mono-BL complex. The same emission energy spectra were obtained, and the emission energy maximum varied by only ±4 nm. The emission quantum yields also remained nearly constant with a variance of only ±2000/400 000 proton counts.

A series of experiments were conducted to search for photochemical substitution in the $Ru\text{–}BL^{2+}$ chelates. Ligand-loss photochemical quantum yields were obtained in acetonitrile in the presence of added $Cl^-$. As reported earlier[44] for related systems, photochemical loss of the BL ligand proceeds according to eq 5. Presumably, substitution occurs by initial $Cl^-$ binding

$$[Ru(bpy)_2BL]^{2+} \xrightarrow[S=CH_3CN]{h\nu,\ Cl^-} [Ru(bpy)_2(Cl)(S)]^+ + BL \qquad (5)$$

followed by thermal loss of the monodentate ligand. The details of photosubstitution of this type are currently under study in our laboratories and will be the subject of a later report. According to the data in Table IV, $[Ru(BL)_3]^{2+}$ shows this photochemical effect more strongly than $[Ru(BL)_2(bpy)]^{2+}$, while $[Ru(bpy)_2BL]^{2+}$ is relatively stable toward ligand loss. It is also noted that ligand loss from $[Ru(BL)_3]^{2+}$ is a factor of 10 larger than bpy loss from $[Ru(bpy)_3]^{2+}$. The relative loss of the BL ligand is consistent with the decreased $\sigma$-bonding ability of the ligand relative to that of bpy. A contributing factor to the photolability of the tris-BL complex may be the bulky nature of the BL ligand.

**Temperature-Dependent Lifetimes and Rate Constants for Excited-State Decay.** Excited-state lifetimes were measured as a function of temperature in a 4:1 (v/v) ethanol–methanol. As shown in Figure 5, excited-state lifetimes are relatively temperature-independent at low temperatures but decrease as the temperature is increased. The data were fit to the expression in eq 6, and the results of the fitting procedures are given in Table V.

$$[\tau_0(T)]^{-1} = k_1 + k_0' \exp[-\Delta E'/RT] \qquad (6)$$

It should be noted that eq 6 forces all the temperature dependence into a single term. Previously Allsopp et al.[45] obtained better curve fits using a double-exponential equation. However, as shown in Figure 5, use of eq 6 gives an excellent fit of the experimental data. The temperature-independent rate constant $k_1$ is the sum of the radiative ($k_r$) and the nonradiative ($k_{nr}$) decay constants for the $^3$MLCT state. The complexes are sufficiently weak emitters that $k_{nr} \approx 1/\tau_0$. Values of $k_r$ were calculated from eq 7,

$$\Phi_r = \eta k_r \tau_0 \qquad (7)$$

where $\eta$ is the efficiency of population of the emitting state(s)

(43) Rillema, D. P.; Nagle, J. K.; Barringer, L. F.; Meyer, T. J. *J. Am. Chem. Soc.* **1981**, *103*, 56.

(44) (a) Grutchley, R. J.; Lever, A. B. P. *J. Am. Chem. Soc.* **1980**, *102*, 7128. (b) Crutchley, R. J.; Lever, A. B. P. *Inorg. Chem.* **1982**, *21*, 2276.

(45) Allsopp, S. R.; Cox, A.; Kemp, T. J.; Reed, W. J. *J. Chem. Soc., Faraday Trans. 1* **1978**, *74*, 1275.

**Table V.** Kinetic Decay Parameters

| compd | $T$,[a] K | $k_1$,[b] $s^{-1}$ | $k_0'$,[b] $s^{-1}$ | $\Delta E'$,[b] $cm^{-1}$ | $k_{nr}$,[c] $s^{-1}$ | $k_r$,[c] $s^{-1}$ |
|---|---|---|---|---|---|---|
| $[Ru(BL)_3]^{2+}$ | 150–298 | $(2.45 \pm 0.04) \times 10^6$ | $(2 \pm 3) \times 10^9$ | $1128 \pm 125$ | $(2.2 \pm 0.3) \times 10^6$ | $(2.7 \pm 0.5) \times 10^5$ |
| $[Ru(BL)_2(bpy)]^{2+}$ | 150–295 | $(1.76 \pm 0.02) \times 10^6$ | $(4 \pm 2) \times 10^9$ | $1417 \pm 55$ | $(1.7 \pm 0.2) \times 10^6$ | $(9.9 \pm 0.5) \times 10^4$ |
| $[Ru(bpy)_2(BL)]^{2+}$ | 150–298 | $(5.41 \pm 0.10) \times 10^5$ | $(2 \pm 8) \times 10^9$ | $789 \pm 300$ | $(4.3 \pm 0.7) \times 10^5$ | $(1.1 \pm 1.0) \times 10^4$ |
| $[Ru(bpy)_3]^{2+}$ [d] | 210–295 | $(6.10 \pm 0.05) \times 10^5$ | $(4 \pm 2) \times 10^{12}$ | $3275 \pm 75$ | $(5.2 \pm 0.5) \times 10^5$ | $(8.0 \pm 1.5) \times 10^4$ |
| $[Ru(bpz)_3]^{2+}$ [d] | 210–295 | $(3.30 \pm 0.03) \times 10^5$ | $(8 \pm 2) \times 10^{12}$ | $3325 \pm 60$ | $(2.4 \pm 0.3) \times 10^5$ | $(9 \pm 1) \times 10^4$ |
| $[Ru(bpz)_2(bpy)]^{2+}$ [d] | 210–345 | $(7.4 \pm 0.1) \times 10^5$ | $(4 \pm 3) \times 10^9$ | $2100 \pm 175$ | $(6.7 \pm 0.7) \times 10^5$ | $(7 \pm 1) \times 10^4$ |
| $[Ru(bpy)_2(bpz)]^{2+}$ [d] | 210–345 | $(2.1 \pm 0.2) \times 10^6$ | $(3 \pm 9) \times 10^7$ | $800 \pm 600$ | $(2.1 \pm 0.2) \times 10^6$ | $(5 \pm 0.5) \times 10^4$ |

[a] Temperature range studied in lifetime experiments. [b] Obtained from temperature-dependent lifetime measurements in the temperature range given. [c] Calculated from $k_1$ above and $\Phi_r$ values from Table IV. [d] Allen, G. H.; White, R. P.; Rillema, D. P.; Meyer, T. J. *J. Am. Chem. Soc.* **1984**, *106*, 2613.

following excitation. The values of $k_r$ in Table V are actually $\eta k_r$, but it is known that $\eta_{isc}$ is unity for $[Ru(bpy)_3]^{2+}$ over a wide range of excitation wavelengths,[46,47] which may be the case here as well. For purposes of comparison, kinetic parameters for an analogous series of complexes containing 2,2'-bipyrazine are included in Table V. The values of $k_r$ and $k_{nr}$ rely on room-temperature data while $k_1$ was determined at <150 °C. While this may result in some uncertainty in their values, $k_r$ and $k_{nr}$ rate constants determined at 7 °C agreed within 10% of those at 25 °C, suggesting that the temperature dependence is a small one.

Data from earlier work[1] have suggested that the temperature-dependent contribution from the $^3$MLCT → dd transition was characterized by $k_0' \approx 10^{12}$–$10^{14}$ $s^{-1}$ and $\Delta E' \approx 2500$–$4000$ $cm^{-1}$. In nonphotochemical systems, the temperature-dependent terms appear to be on the order of $k_0' \approx 10^7$–$10^8$ $s^{-1}$ and $\Delta E' \approx 400$–$1000$ $cm^{-1}$, which were attributed to population and decay from a low-lying MLCT state with greater singlet character.

The ratio $[k_0' \exp(-\Delta E'/RT)]/[k_1 + k_0' \exp(-\Delta E'/RT)]$ gives the fraction of energy that is dissipated from the thermally activated processes that lead to decay. For $[Ru(BL)_3]^{2+}$ this ratio corresponds to 83% of excited-state decay at room temperature, 72% for $[Ru(BL)_2(bpy)]^{2+}$, and 99% for $[Ru(bpy)_2(BL)]^{2+}$. While the temperature dependence in eq 6 has been forced into the exponential term, additional contributions to the temperature dependence could come from $k_1$.

Since the energy gap law, given in eq 8,[48] has been shown to apply to nonradiative decay in related complexes[48,49] and since experimentally $k_1 \approx k_{nr}$, it follows that $\ln k_1 \propto E_0$. If $E_0$ is

$$\ln k_{nr} = \left[ \ln \beta_0 - S_M + (\gamma + 1)^2 \left( \frac{\Delta \bar{\nu}_{1/2}}{\hbar \omega_M} \right)^2 / 16 \ln 2 \right] - \left( \frac{\gamma_0 E_0}{\hbar \omega_M} \right) \quad (8)$$

temperature dependent, a temperature dependence is induced in $k_1$ at the glass-to-fluid transition as shown by recent experiments in 4:1 ethanol–methanol.[50] However, shifts in $E_0$ from −130 °C to room temperature indicate that the effect is negligible.

The temperature dependence may arise from (1) the transition between the BL-based and bpy-based MLCT states ($^3$MLCT(BL) → $^3$MLCT(bpy)), (2) population of a fourth MLCT state having greater singlet character than the lower three, (3) population of the third MLCT state lying ~1000 $cm^{-1}$ above the other two as rationalized by the "localized orbital" model[18c,51] for mixed-ligand complexes, and (4) population and decay of the low-lying dd states. The MLCT(BL) to MLCT(bpy) transition $(d\pi)^5(\pi^*)^1$(BL) → $(d\pi)^5(\pi^*)^1$(bpy) followed by bpy-based MLCT decay can be ruled out on the basis of the energy requirement involved. The energy gap between the $^3$MLCT(BL) and $^3$MLCT(bpy) states is on the order of 0.7 V (~5600 $cm^{-1}$) as judged by the difference in redox potentials (i.e. $E_{1/2}$ for $[Ru(bpy)_3]^{2+/+}$ is −1.31 V and for $[Ru(BL)_3]^{2+/+}$ is −0.60 V) and is too large to account for $\Delta E'$.

The "$^3$MLCT" state has been shown[11c,52] to consist of a series of three closely spaced states with a spacing between them of ~10 and ~50 $cm^{-1}$ for $[Ru(bpy_3)]^{2+}$. For $[Os(bpy)_3]^{2+}$, evidence exists for the presence of the fourth state ~600 $cm^{-1}$ above the $^3$MLCT states.[45,53] A recent theoretical treatment for the complexes predicts the existence of an additional MLCT state having a greater degree of singlet character than the lower three $^3$MLCT states.[13e] One limiting interpretation of the temperature dependence is that $\Delta E'$ is the energy gap to the fourth state and $k_0'$ is the rate constant for the decay of that state. From Table V for $[Ru(bpy)_2BL]^{2+}$, $k_0'$ (~$10^9$ $s^{-1}$) is significantly greater than $k_1$ (~$5 \times 10^5$ $s^{-1}$), which is consistent with enhanced singlet character for the higher state. Population and decay from a fourth MLCT state may account for excited-state decay in $[Ru(bpy)_2BL]^{2+*}$ due to the low $\Delta E'$ value and the fact that little photochemistry is observed ($\Phi_p < 10^{-4}$). Similar arguments could be made for the situation as described by the localized-orbital model, which places the third MLCT state for mixed-ligand complexes ~1000 $cm^{-1}$ above the other two.[51] The large value for the fraction $[k_0' \exp(-\Delta E'/RT)]/[k_1 + k_0' \exp(-\Delta E'/RT)]$ implies that 99% of the decay is from this state at room temperature.

For $[Ru(BL)_3]^{2+}$ and $[Ru(BL)_2(bpy)]^{2+}$, the situation is less clear. $[Ru(BL)_3]^{2+}$ is photochemically active whereas $[Ru(bpy)_2(BL)]^{2+}$ shows little activity. $[Ru(BL)_2(bpy)]^{2+}$ displays intermediate photochemical substitution quantum yields at about half the level found for $[Ru(bpy)_3]^{2+}$. Earlier it was suggested that the decay parameters for the thermally activated path might be indicative of different kinetic limits for dd population and decay; i.e., $k_0' = 10^{12}$–$10^{14}$ $s^{-1}$ and $\Delta E' > 2500$ $cm^{-1}$ indicative of irreversible MLCT → dd surface crossing for compounds as found for $[Ru(bpy)_3]^{2+}$, $[Ru(bpz)_3]^{2+}$, and $[Ru(bpm)_3]^{2+}$ and $k_0' \approx 10^7$ $s^{-1}$ and $\Delta E' \approx 2000$ $cm^{-1}$ indicative of an equilibrium between the dd and $^3$MLCT states followed by dd decay as found for $[Ru(bpz)_2(bpy)]^{2+}$. For $[Ru(BL)_3]^{2+}$ and $[Ru(BL)_2(bpy)]^{2+}$, $k_0' \approx 10^9$ $s^{-1}$ and $\Delta E' \approx 1100$–$1400$ $cm^{-1}$, which fall between the parameters for dd ⇄ $^3$MLCT and population of an upper MLCT state, and we may be observing contributions from both types of processes.

In a comparison of $k_1$ for the three BL complexes, the change in $E_0$ is small but it is notable that the trend is opposite to that predicted by the energy gap law. The reason for this anomaly is unknown but may be related to stronger ligand field perturbation of the ligand $\pi^*$ orbitals.

**Emission Spectra.** The emission spectrum of $[Ru(BL)_2(bpy)]^{2+}$ at 90 K is shown in Figure 6 along with the results of a spectral fitting procedure described earlier[35] based on the parameters $E_{00}$, $S_M$, $\hbar\omega_M$, $S_L$, $\hbar\omega_L$, and fwhm. $E_{00}$ is the 0–0 energy, $S_M$ and $\hbar\omega_M$ are respectively the electron-vibrational coupling constant and vibrational spacing of seven to eight medium-frequency $\nu$(poly-

(46) Demas, J. N.; Taylor, D. G. *Inorg. Chem.* **1979**, *18*, 3177.
(47) (a) Bensason, R.; Salet, C.; Balzani, V. *J. Phys. Chem.* **1976**, *80*, 2499. (b) Boletta, F.; Juris, A.; Mestri, M.; Sandrini, D. *Inorg. Chim. Acta* **1980**, *44*, L175.
(48) Kober, E. M.; Caspar, J. V.; Lumpkin, R. S.; Meyer, T. J. *J. Phys. Chem.* **1986**, *90*, 3722.
(49) (a) Caspar, J. V.; Meyer, T. J. *Inorg. Chem.* **1983**, *22*, 2044. (b) Meyer, T. J. *Prog. Inorg. Chem.* **1983**, *30*, 389–440.
(50) Lumpkin, R. S.; Meyer, T. J. *J. Phys. Chem.* **1986**, *90*, 5307.
(51) DeArmond, M. K.; Hanck, K. H.; Wertz, D. W. *Coord. Chem. Rev.* **1985**, *64*, 65.
(52) Allsopp, S. R.; Cox, A.; Kemp, T. J.; Reed, W. J.; Carasitti, V.; Traverso, O. *J. Chem. Soc., Faraday Trans. 1* **1979**, *75*, 353.
(53) Cealemans, A.; Vanquickenborne, L. G. *J. Am. Chem. Soc.* **1981**, *103*, 2238.

**Table VI.** Emission Data and Emission Spectral Fitting Parameters in 4:1 (v/v) Ethanol–Methanol Glasses

| compd | $E_{00}$,[a] cm$^{-1}$ | $\hbar\omega_M$,[a,b] cm$^{-1}$ | $S_M$[a,c] | $\hbar\omega_L$,[a,d] cm$^{-1}$ | $S_L$[a,e] | fwhm,[a] cm$^{-1}$ |
|---|---|---|---|---|---|---|
| $[Ru(BL)_3]^{2+}$[f] | 14 700 | 1230 | 0.69 | 300 | 2.30 | 650 |
| $[Ru(BL)_2(bpy)]^{2+}$[g] | 14 400 | 1230 | 0.62 | 300 | 2.56 | 660 |
| $[Ru(bpy)_2(BL)]^{2+}$[h] | 14 300 | 1230 | 0.55 | 300 | 2.20 | 670 |
| $[Ru(bpy)_3]^{2+}$[i] | 17 400 | 1400 | 0.95 | 400 | 1.10 | 580 |
| $[Ru(bpz)_3]^{2+}$ | 17 600 | 1300 | 0.95 | 300 | 1.48 | 650 |
| $[Ru(bpz)_2(bpy)]^{2+}$[i] | 16 800 | 1200 | 1.35 | 400 | 1.50 | 650 |
| $[Ru(bpy)_2(bpz)]^{2+}$[i] | 15 700 | 1300 | 0.90 | 400 | 1.25 | 650 |

[a] Spectral fitting parameters obtained from a two-mode fitting procedure or data obtained over the temperature range indicated in 4:1 (v/v) ethanol–methanol glasses. Errors: ±5% for $E_{00}$, $\hbar\omega_M$, $S_M$, and fwhm; ±10% for $\hbar\omega_L$ and $S_L$. [b] Ring stretches. [c] Ring stretch distortions. [d] Metal–ligand stretching vibrations. [e] Metal–ligand stretch distortions. [f] 90 K. [g] 87 K. [h] 93 K. [i] 77 K. Data from: Allen, G. H.; White, R. P.; Rillema, D. P.; Meyer, T. J. *J. Am. Chem. Soc.* **1984**, *100*, 2613. The values for $[Ru(bpz)_3]^{2+}$ were calculated from this reference.

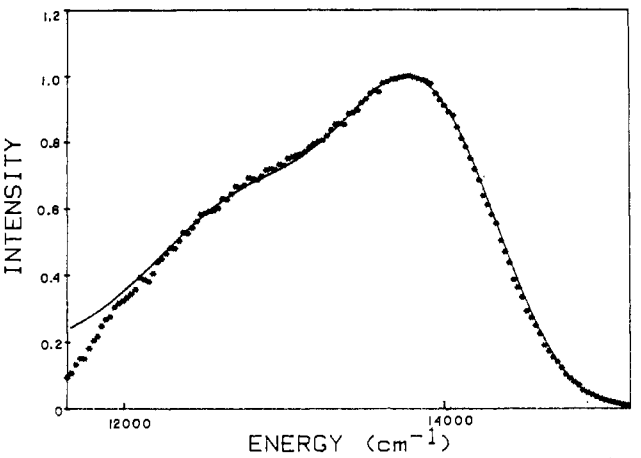


**Figure 6.** Emission data (*) at 90 K in a 4:1 EtOH–MeOH glass and calculated fit (—) using the spectral parameters in Table VI for $[Ru(BL)_2(bpy)]^{2+}$.

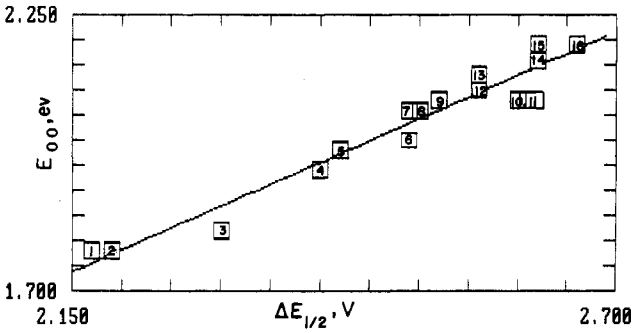


**Figure 7.** Plot of $E_{00}$ as a function of the energy gap $\Delta E_{1/2}$, where $\Delta E_{1/2}$ is $E_{1/2}{}^{3+/2+} - E_{1/2}{}^{2+/+}$. Compounds: (1) $Ru(bpy)(BL)^{2+}$; (2) $Ru(BL)_2(bpy)^{2+}$; (3) $Ru(BL)_3^{2+}$; (4) $Ru(bpy)_2(bpz)^{2+}$; (5) $Ru(bpy)_2(bpm)^{2+}$; (6) $Ru(bpy)(bpz)(bpm)^{2+}$; (7) $Ru(4,4'\text{-DCE})_3^{2+}$; (8) $Ru(bpm)_2(bpy)^{2+}$; (9) $Ru(5,5'\text{-DEA})_3^{2+}$; (10) $Ru(bpm)_3^{2+}$; (11) $Ru(bpz)_2(bpy)^{2+}$; (12) $Ru(4,4'\text{-DEA})_3^{2+}$; (13) $Ru(4,4'\text{-Me})_3^{2+}$; (14) $Ru(bpy)_3^{2+}$; (15) $Ru(bpz)_2(bpm)^{2+}$; (16) $Ru(bpz)_3^{2+}$. Data for entries 7, 9, 12, and 13 are from unpublished observations of Paul Neveau. Abbreviations used that were previously undefined are as follows: bpm, 2,2′-bipyrimidine; 4,4′-DCE, 4,4′-dicarboxy-2,2′-bipyridine ethyl ester; 4,4′-DEA, 4,4′-bis(diethylamino)-2,2′-bipyridine; 5,5′-DEA, 5,5′-bis(diethylamino)-2,2′-bipyridine; 4,4′-Me, 4,4′-dimethyl-2,2′-bipyridine.

pyridyl) ring stretching modes, $S_L$ and $\hbar\omega_L$ are the corresponding quantities for an average of a series of low-frequency contributors, and fwhm is the full width at half-maximum for a series of individual vibrational contributors. In the emission spectra, vibrational progressions can be seen giving good initial estimates for $\hbar\omega_M$; $S_M$ can readily be estimated from peak heights of the first two components. A major contribution to $S_L$ is from metal to ligand stretching modes in the 250–400-cm$^{-1}$ region. However, low-frequency stretching progressions are not observed at 80–90 K, where the spectra were acquired, although they must be included to obtain satisfactory fits. Consequently, we have set $\hbar\omega_L$ to 300 cm$^{-1}$ and varied $S_L$ and fwhm. The best-fit values for the parameters obtained by spectral fitting are summarized in Table VI, where they are compared to those obtained earlier for related complexes.

The lower $S_M$ values for the BL-based MLCT excited states are not unexpected, since earlier work has shown that $S_M$ decreases as $E_{00}$ decreases.[35,48] $S_M$ is related to the decay in equilibrium displacement between the ground and excited states ($\Delta Q_{eq}$) by $S_M = 1/2(M\omega/\hbar)(\Delta Q_{eq})^2$, where $M$ is the reduced mass and $\omega$ is the angular frequency. The variation of $S_M$ and $\Delta Q_{eq}$ with $E_{00}$ can be reconciled as arising from increased distortions of higher energy excited states where the extent of charge transfer is greater.[35,48] The $S_M$ values are sufficiently low that contributions may be occurring from both the second and third $^3$MLCT states with $S_M$ increasing at higher $T$ as the third state becomes fully populated and begins to dominate the emission. As for other low-energy emitters, $\hbar\omega_M$ is low and may reflect the increasingly more important contributions from the lower energy $\nu$(BL) ring stretching modes to the averaged vibrational parameter as $E_{00}$ decreases.

The increase in $S_L$ for BL compared to the values for the other chromophoric ligands may be real with greater M–L distortions occurring because BL is a weaker $\sigma$ donor ligand. The full width at half-maximum (fwhm) of the 0–0 vibronic component is fairly constant through the series of chromophoric ligands and indicates that the outer-sphere trapping energy $\chi_0$ for the electron-transfer process associated with the excited-state to ground-state conversion is fairly constant.

A plot of $E_{00}$ vs. $\Delta E_{1/2}$, where $\Delta E_{1/2} = E_{1/2}{}^{3+/2+} - E_{1/2}{}^{2+/+}$, is shown in Figure 7. The plot is linear with a slope of 0.87, a correlation coefficient of 0.97, and an intercept of −0.13. The comparisons made in Figure 7 include examples of ruthenium compounds containing bipyrazine, bipyrimidine, bipyridine, 2,3-bis(2-pyridyl)quinoxaline, and several substituted-bipyridine ligands.[1,54] The complexes chosen are ones with known $E_{00}$ values as determined by spectral fitting. The basis for the comparison is the expected relationship between $\Delta E_{1/2}$ and $E_{00}$, where $\Delta E_{1/2}$ is the outer-sphere analogue[2] of the intramolecular emission experiment as indicated in eq 9 and 10.

$$[(AA^-)Ru^{II}L_4]^+ + [(AA)Ru^{III}L_4]^{3+} \xrightarrow[\Delta E_{1/2}]{} 2[(AA)Ru^{II}L_4]^{2+} \quad (9)$$

$$[(AA^-)Ru^{III}L_4]^{2+*} \xrightarrow[E_{00}]{} [(AA)Ru^{II}L_4]^{2+} \quad (10)$$

The correlation, which extends over a broad potential range and includes a series of different polypyridyl-based chromophores, is clearly impressive. It verifies the MLCT nature of emitting excited states and demonstrates the utility of electrochemical data in estimating excited-state energies. The nearly unit slope is notable in showing that the same factors at the molecular level that influence $\pi^*$ acceptor and $d\pi$ donor levels are carried over to the excited state. An important contributor to the near-unit slope and non-zero intercept of the correlation is the existence of significant electrostatic interaction between the excited electron and the $(d\pi)^5$ core, an interaction that does not exist in the electrochemical experiment.

(54) Neveau, P. Ph.D. Thesis, The University of North Carolina, 1986.

In related work it has been noted that correlations of this type but with $E_{em}$ rather than $E_{00}$ gave correlations that are statistically less significant and slopes that are far less.[2,3a] The major difference between the correlations with $E_{em}$ and $E_{00}$ is that $E_{em}$ includes contributions from the vibrational modes, which vary as $E_{00}$.

**Acknowledgment.** This research was sponsored, in part, by the Division of Chemical Sciences and the Division of Material Sciences, Office of Basic Energy Sciences, U.S. Department of Energy. Materials Sciences sponsorship was under Contract DE-ACO-5-84OR21400 with Martin-Marietta Energy Systems, Inc. D.S.J. acknowledges support from the Foundation of The University of North Carolina at Charlotte and from the Oak Ridge Associated Universities under Participation Agreement No. S-1765. D.P.R. also thanks the Keenan Foundation for a Visiting Professorship Position during the fall of 1984.

**Supplementary Material Available:** Listings of displacement parameters, bond lengths, and bond angles (8 pages). Ordering information is given on any current masthead page.

Contribution from the Laboratoire de Chimie de Coordination, Unité 8241 liée par convention à l'Université Paul Sabatier, 31077 Toulouse Cedex, France

# Cluster-Promoted Cleavage of a Phosphorus–Carbon Bond under Ambient Conditions. Synthesis, Structure, and Stereospecific Substitution Reactions of the Acyl Cluster Complex $Ru_3(\mu\text{-}\eta^2\text{-}C(O)(C_6H_5))(\mu_3\text{-}\eta^2\text{-}P(C_6H_5)(C_5H_4N))(CO)_9$

Noël Lugan, Guy Lavigne, and Jean-Jacques Bonnet*

*Received July 17, 1986*

The monosubstituted complex $Ru_3(CO)_{11}(PPh_2py)$ (**1**), prepared from $Ru_3(CO)_{12}$ and diphenylpyridylphosphine $PPh_2py$ by using [PPN]CN as a catalyst, experiences a spontaneous P–C bond-cleavage reaction at 25 °C. The expelled phenyl substituent undergoes migratory CO insertion to yield the acyl complex $Ru_3(\mu\text{-}\eta^2\text{-}C(O)(C_6H_5))(\mu_3\text{-}\eta^2\text{-}P(C_6H_5)(C_5H_4N))(CO)_9$ (**2**) (yield, 85%). The high reactivity observed for **2** is related to a stereospecific labilizing effect of the acyl group toward adjacent carbonyl ligands. This is exemplified by its reaction with several phosphines at 30 °C, leading to $Ru_3(\mu\text{-}\eta^2\text{-}C(O)(C_6H_5))(\mu_3\text{-}\eta^2\text{-}P(C_6H_5)(C_5H_4N))(CO)_8(L)$ (**3**) (**3a**, L = $PPh_3$; **3b**, L = $PPh_2H$; **3c**, L = $PCy_2H$). The X-ray structures of **2** and **3a** are reported. Crystal data for $Ru_3(\mu\text{-}\eta^2\text{-}C(O)(C_6H_5))(\mu_3\text{-}\eta^2\text{-}P(C_6H_5)(C_5H_4N))(CO)_9$ (**2**): orthorhombic, space group $P2_12_12_1$, $a$ = 10.431 (2) Å, $b$ = 15.888 (5) Å, $c$ = 17.821 (5) Å, $V$ = 2953 Å$^3$, $Z$ = 4. Full-matrix least-squares refinement of 379 variables for 2757 reflections with $F_o^2 > 3\sigma(F_o^2)$ led to $R$ = 0.043 and $R_w$ = 0.049. Crystal data for $Ru_3(\mu\text{-}\eta^2\text{-}C(O)(C_6H_5))(\mu_3\text{-}\eta^2\text{-}P(C_6H_5)(C_5H_4N))(CO)_8(P(C_6H_5)_3)$ (**3a**): monoclinic, space group $P2_1/n$, $a$ = 10.650 (3) Å, $b$ = 31.023 (4) Å, $c$ = 13.016 (2) Å, $\beta$ = 97.57(2)°, $V$ = 4262 Å$^3$, $Z$ = 4. Full-matrix least-squares refinement of 383 variables for 5770 observations with $F_o^2 > 3\sigma(F_o^2)$ led to $R$ = 0.049 and $R_w$ = 0.087. Both these triangular 50-e cluster complexes are edge double-bridged species, with an acyl group $C(O)(C_6H_5)$ and a phenylpyridylphosphido group $P(C_6H_5)(C_5H_4N)$ spanning the open metal–metal vector Ru(2)-Ru(3). Additional coordination of the nitrogen atom of the pyridyl substituent on phosphorus to the unique ruthenium atom Ru(1) confers on the latter ligand a key role in preserving the integrity of the metal cluster. In the monosubstituted derivatives **3**, the phosphine ligand occupies an equatorial coordination site, in a cis position relative to the oxygen of the acyl group.

## Introduction

Recent years have seen considerable success in various attempts to bring about the reaction of clusters under mild conditions.[1] For a long time, investigators in ruthenium cluster chemistry have been looking for ruthenium complexes able to duplicate the rich chemistry available to osmium through reactive species, either unsaturated, like $Os_3(\mu\text{-}H)_2(CO)_{10}$,[2] or lightly stabilized, like $Os_3(CO)_{12-n}(CH_3CN)_n$ ($n$ = 1, 2).[3] Success has been recently obtained in the preparation of $Ru_3(CO)_{12-n}(CH_3CN)_n$,[4] permitting the activation of various substrates at or below ambient temperature. Alternately, discoveries of catalytic systems[5-7] for substitution of CO by phosphine ligands in $Ru_3(CO)_{12}$ have provided a rapid and quantitative access to monosubstituted cluster complexes $Ru_3(CO)_{11}(PR_3)$, which were not readily available in high yield through thermal routes.

Following our recent studies of the cluster-assisted transformations of bis(diphenylphosphino)methane,[8,9] we used diphenylpyridylphosphine as an alternate edge-bridging ligand, with the aim to induce a site specificity within a ruthenium triangle. Earlier studies[10] of the thermal reaction of this ligand with $Ru_3(CO)_{12}$ led to isolation of the trisubstituted complex $Ru_3(CO)_9(PPh_2py)_3$ (along with monomeric species), in agreement with previous observations that monosubstitution is the rate-determining step.[11] By using published catalytic procedures,[5,6] we were able to isolate the monosubstituted derivative $Ru_3(CO)_{11}(PPh_2py)$ (**1**) quantitatively. This species is the precursor for the title complex $Ru_3(\mu\text{-}\eta^2\text{-}C(O)(C_6H_5))(\mu_3\text{-}\eta^2\text{-}P(C_6H_5)(C_5H_4N))(CO)_9$ (**2**). Though electronically saturated, this complex possesses important features that one would like to design into a cluster:

(1) Lavigne, G.; Kaesz, H. D. In *Clusters and Catalysis*; Gates, B. C.; Guczi, L., Knözinger, H., Eds.; Elsevier: Amsterdam, 1986; Chapter IV.
(2) Adams, R. D.; Selegue, J. P. In *Comprehensive Organometallic Chemistry*; Wilkinson, G., Stone, F. G. A., Abel, E. W., Eds.; Pergamon: Oxford, England, 1982; Vol. IV, p 1023.
(3) (a) Tachikawa, M.; Shapley, J. R. *J. Organomet. Chem.* **1977**, *124*, C19. (b) Shapley, J. R.; Pearson, G. A.; Tachikawa, M.; Schmüdt, G. E.; Churchill, M. R.; Hollander, F. J. *J. Am. Chem. Soc.* **1977**, *99*, 8064. (c) Johnson, B. F. G.; Lewis, J.; Pippard, D. A. *J. Chem. Soc., Dalton Trans.* **1981**, 407. (d) Dawson, P. A.; Johnson, B. F. G.; Lewis, J.; Puga, J.; Raithby, P. R.; Rosales, M. J. *J. Chem. Soc., Dalton Trans.* **1982**, 233.
(4) Foulds, G. A.; Johnson, B. F. G.; Lewis, J. *J. Organomet. Chem.* **1985**, *296*, 147.
(5) Bruce, M. I.; Matisons, J. G.; Nicholson, B. K. *J. Organomet. Chem.* **1983**, *247*, 321.
(6) (a) Lavigne, G.; Kaesz, H. D. *J. Am. Chem. Soc.* **1984**, *106*, 4647. (b) The catalytic system involving highly dissociated salts has recently been elucidated and extended to the case of $[PPN]BH_4$ and various hydride donors: Lavigne, G.; Lugan, N.; Bonnet, J. J., submitted for publication.
(7) Aime, S.; Botta, M.; Gobetto, R.; Osella, D. *Organometallics* **1985**, *4*, 1475.
(8) Lugan, N.; Bonnet, J.-J.; Ibers, J. A. *J. Am. Chem. Soc.* **1985**, *107*, 4484.
(9) Bergounhou, C.; Bonnet, J.-J.; Fompeyrine, P.; Lavigne, G.; Lugan, N.; Mansilla, F. *Organometallics* **1986**, *5*, 60 and references therein.
(10) Maisonnat, A.; Farr, J. P.; Olmstead, M. M.; Hunt, C.; Balch, A. L. *Inorg. Chem.* **1982**, *21*, 3961.
(11) (a) Candlin, J. P.; Shortland, A. C. *J. Organomet. Chem.* **1969**, *16*, 289. (b) Poë, A.; Twigg, M. V. *J. Chem. Soc., Dalton Trans.* **1974**, 1860. (c) Keeton, D. P.; Malik, S. K.; Poë, A. *J. Chem. Soc., Dalton Trans.* **1977**, 233. (d) Malik, S. K.; Poë, A. *Inorg. Chem.* **1978**, *17*, 1484.

0020-1669/87/1326-0585$01.50/0 